Flexible Radar Front End with Multimodal Transition at 300 GHz

Martin Geiger[1*], Simon Gut[1], Philipp Hügler[1], and Christian Waldschmidt[1]
[1] Insitute of Microwave Engineering, Ulm University, 89081 Ulm, Germany
[*]martin-2.geiger@uni-ulm.de

***Abstract* — Especially for short-range radar sensors, a protection of the electronics against environmental damage like heat or humidity as well as a robust antenna front end are essential. In order to separate the sensitive electronics and the robust antenna spatially, a system concept for a 300-GHz radar with mechanically flexible front end is presented in this paper. The flexible front end is realized with a low-loss dielectric waveguide (DWG) with losses of around 15 dB/m. It is bendable up to a radius of 1 cm. An elliptical lens (30.9 dBi) at the end is used to focus the beam. The front end is fed by a radar MMIC in a QFN-like package with an integrated silicon lens. The wide beam is focused by simply placing a multimodal DWG above package and lens. The intentionally caused interference of the individual modes then results in a field maximum in the center, and the fundamental mode can be fed into the DWG.**

***Keywords* — dielectric waveguide, flexible radar sensor, integrated lens antenna, multimode interference, mm-wave radar.**

I. Introduction

The demand for low-cost and compact radar systems increases due to their robust performance in distance and velocity measurements. Advances in the SiGe technology are pushing this progress and enabling the realization of cheap monolithic microwave integrated circuits (MMIC) and radar systems from 100 GHz even up to the lowest THz range [1]–[3]. The large available absolute bandwidth results in a high range resolution and a superior short-range radar performance compared to radars at 24 GHz and 77 GHz.

However, a very good short-range performance in harsh environmental conditions and a compact design with susceptible electronics is a contradiction in terms. Since the electronics have limitations at high temperatures or in dirty, humidity, and explosive environments, the requirements for the sensor housing are high. These in turn limit the performance of a radar or even make the use of it unfavorable.

In order to avoid these problems, a 160-GHz radar with flexible front end was presented in [4] to spatially separate electronics on the printed circuit board (PCB) and antenna. This results in a radar sensor with a compact and arbitrarily movable antenna, which can be used flexibly for various applications [5], [6]. The front end of this system is realized with a very low-loss dielectric waveguide (DWG) which also enables a signal distribution over longer distances. A multi-component construction with DWGs, superstrate antennas, and metallic waveguides is used to connect the MMIC and the flexible front end. Not only the metallic waveguide components are expensive, but also the assembly of the components is complex and must be made highly precise.

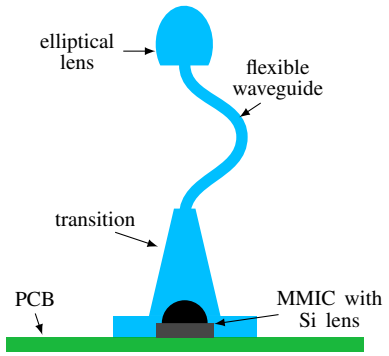

Fig. 1. System concept for a sniffer probe at 300 GHz.

With increasing frequency, the required packaging accuracy also increases and the approach is no longer applicable. This paper presents an improved system concept for a radar with flexible front end. The expensive metallic waveguide components are omitted and the MMIC in a standard QFN-like package with integrated silicon lens antenna [1], [7] is directly connected to the DWG. The interconnection encases the package completely and is simply aligned to it. In the following section, the overall system concept based on a 300-GHz MMIC is explained. Afterwards, the individual components and measurement results are presented in more detail.

II. System Concept

The proposed system concept is shown in simplified form in Fig. 1. The sniffer probe is based on a 300-GHz radar MMIC in a QFN-like package with a silicon lens. In order to focus the radiated power, a transition made of high-density polyethylene (HDPE) is placed directly above the lens and encases the package completely. The design principle of this transition is based on multimodal interference in DWGs. The flexible front end is realized with a DWG feeding a high-gain elliptical lens antenna.

III. 300-GHz Radar MMIC

The radar MMIC is a fully integrated SiGe transceiver with on-chip antenna for FMCW radar applications. The chip architecture is based on a 75-GHz VCO, whose output signal is quadrupled and thus, a bandwidth up to 41.5 GHz is achieved. The MMIC is in a QFN-like package and has an on-chip bowtie antenna as shown in Fig. 2. The bowtie antenna is on the top layer of the SiO_2 substrate and radiates through the substrate and the silicon bulk ($\varepsilon_r = 11.9$, $\rho = 50\,\Omega\,\mathrm{cm}$).

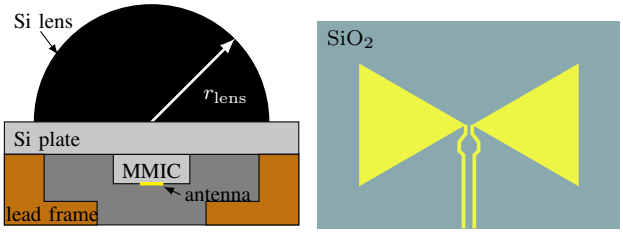

(a) (b)

Fig. 2. (a) Simplified cross-section of the MMIC package and (b) a more detailed view on the antenna layout.

The MMIC is glued on a plate made of silicon with similar electrical properties. A high-resistivity silicon lens ($\varepsilon_r = 11.9$, $\rho > 1\,\text{k}\Omega\,\text{cm}$) with a radius $r_{\text{lens}} = 2.25\,\text{mm}$ is placed on the plate to focus the beam [7]. The antenna has a simulated efficiency of around 45 % due to the high substrate losses in the bulk and the silicon plate and the reflection at the lens surface.

IV. Transition

In order to feed the flexible front end with the radar MMIC a transition from the QFN package to the DWG is needed. The transition should focus the radiated power without modifying the package or the on-chip antenna. Furthermore, the assembly should be as simple as possible with low accuracy requirements.

The design of the transition is based on a physical feature called multimode interference, well known from optics for an efficient design of couplers [8], [9]. The input field distribution is repeated periodically in a multimodal waveguide with constant dimensions along the propagation direction and can be reproduced to single or multiple images of the input field. In the design of the transition, this basic idea is adopted in order to adapt the radiated field distribution of the silicon antenna to the fundamental mode of the DWG by stepwise tapering the transition.

The radiated field distribution $\Psi(x, y, 0)$ of the antenna can be expressed as the sum of the m individual propagating modes $\psi(x, y)$ in the DWG with the weighting factor c_n to

$$\Psi(x, y, 0) = \sum_{n=0}^{m-1} c_n \psi_n(x, y). \tag{1}$$

Due to the different propagation constants β_n of each mode the field distribution along the propagation direction is given by

$$\Psi(x, y, z) = \sum_{n=0}^{m-1} c_n \psi_n(x, y) \mathrm{e}^{\mathrm{j}(\beta_0 - \beta_n) z}. \tag{2}$$

Thus, the field distribution changes along the propagation direction z depending on the superposition of the modes.

In order to realize this transition, a large DWG is placed above the package and the lens. Since the package has a dimension of $5\,\text{mm} \times 5\,\text{mm}$, a large number of modes is propagable and the field distribution must be strongly focused to feed a single mode DWG with a cross-section of

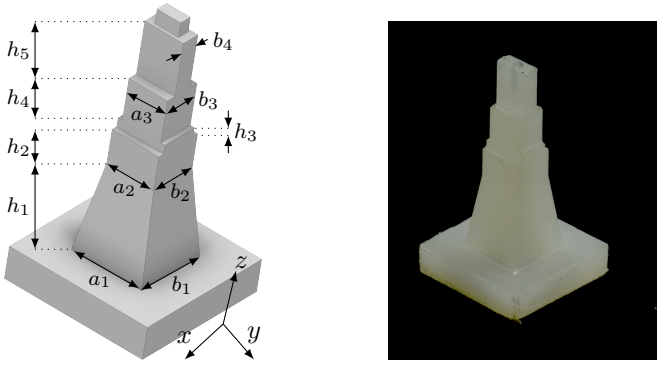

(a) (b)

Fig. 3. 3D view on the transition from MMIC to DWG with dimensions.

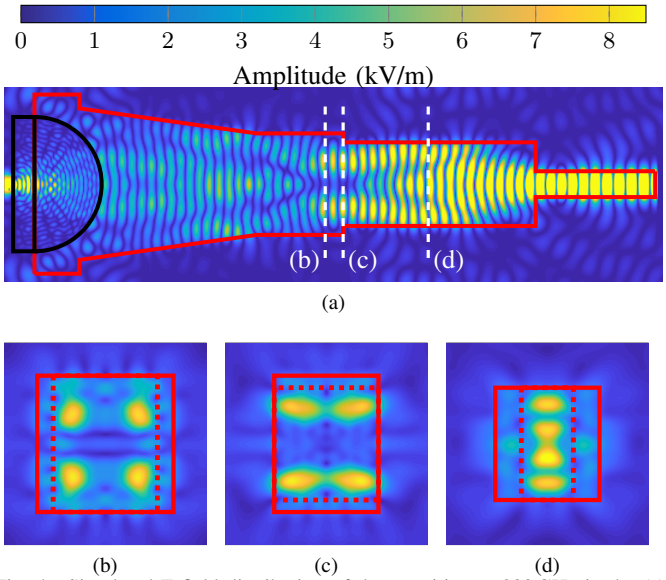

(a)

(b) (c) (d)

Fig. 4. Simulated E-field distribution of the transition at 300 GHz in the (a) H-plane and in the $x-y$-plane at the three steps with both cross-sections in red (continuous and dotted).

$432\,\mu\text{m} \times 864\,\mu\text{m}$. Due to the large number of modes the direct focusing is almost impossible and would require a very long transition resulting in high dielectric losses.

In order to reduce the number of modes and the losses, the cross-section is reduced by a taper and steps as shown in the model in Fig. 3(a). In the bottom part of the transition an almost plane wave propagates in the dielectric medium. The radiated field of the antenna can be concentrated with a taper of height h_1. Above the taper, the cross-section is reduced stepwise. Since several modes are propagating in the dielectric, they interfere with each other. As soon as the field distribution is more concentrated in the center, the cross-section is reduced by a certain width. To visualize the mode reduction, the field distribution in the H-plane (a) and in the x-y plane (b)–(d) of the transition is shown in Fig. 4.

The simulated insertion loss of the transition is around −5.5 dB below 315 GHz and decreases to −7.5 dB at 330 GHz as shown in Fig. 5. A more detailed investigation on the losses of the transition shows that some of the power is radiated sideways and downwards, and only power in the angular range

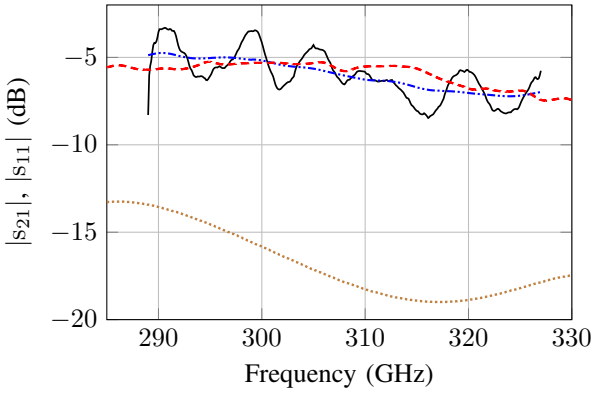

Fig. 5. Simulated ($|s_{11}|$ (·····), $|s_{21}|$ (- - - -)) and measured ($|s_{21}|$ (——)) S-parameters for the transition from MMIC to DWG. The mean value of the transition loss (-·-·-) is also shown.

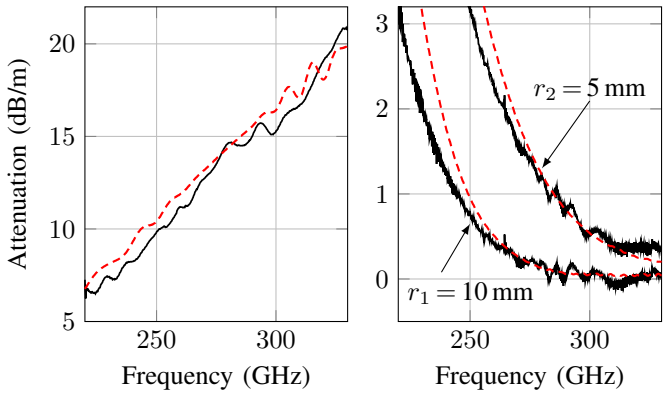

(a) (b)

Fig. 6. Simulated (- - - -) and measured (——) attenuation for (a) a straight DWG and (b) a DWG with a 180° bend.

Table 1. Dimensions for the transition in µm.

a_1	5076	b_1	5076	h_1	5937
a_2	3400	b_2	3400	h_2	2300
a_3	2800	b_3	2600	h_3	600
a_4	864	b_4	1300	h_4	2850
		b_5	864	h_5	3600

of maximum −45° to 45° is captured by the DWG transition. This results in an insertion loss caused by the MMIC and the package setup of around −4 dB due to radiation losses and material losses. Consequently, the multimodal DWG based transition causes an additional insertion loss of only −1.5 dB. The matching of the transition is mainly determined by the matching of the bowtie antenna. The simulated $|s_{11}|$ has a center frequency of 317 GHz and is below −10 dB in the entire used frequency range.

One advantage of the transition is the reduced accuracy requirements of the transition itself compared to resonators or patch antennas. These structures need an accuracy below 10 µm, whereas the requirements of the proposed transition are above 100 µm. Also the assembly can be done without a complex alignment. The transition is aligned with the package with a positioning accuracy of around 50 µm resulting in additional losses below 0.3 dB.

Since the transition is simply placed over the package with the integrated lens, it is also possible to carry out radar measurements with and without a flexible front end using the same MMIC package. A cavity inside the transition fits positively to the MMIC with lens to avoid gaps which would cause additional reflections. The transition as well as the DWG are made of HDPE ($\varepsilon_r = 2.3$, $\tan\delta = 5 \cdot 10^{-4}$ at 300 GHz). The dimensions are listed in Table 1 and a photo is shown in Fig. 3(b).

For the determination of the transmission loss of the transition the output power of the flexible front end was measured and compared to the output power on-chip before the bowtie antenna. Therefore, a transition from DWG to metallic waveguide was designed to measure the power with a VNA. The measured transmission loss from MMIC to DWG is shown in Fig. 5. Compared to the simulations, ripples are caused by standing waves in the multimodal transition and in the transition to the metallic waveguide. However, the measured mean value is in good agreement with the simulation.

V. Flexible Front End

The flexible front end of the radar system with the DWG and the elliptical lens antenna is comparable to the presented system in [4]. However, all components have to be adapted to the higher frequency and the larger bandwidth.

The DWG is the flexible part of the radar system. The fundamental HE_{11} mode is excited by the transition from the MMIC. The field distribution of the mode depends on the permittivity and the DWG dimensions. These parameters have to be considered in the design to minimize dielectric and radiation losses. The dispersion of the DWG is a further design aspect due to the large available bandwidth of 41.5 GHz.

The designed DWG has a rectangular cross-section of 432 µm × 864 µm and is made of HDPE. This results in a dielectric loss of about 15 dB/m at 300 GHz as shown in Fig 6(a). Due to the strongly concentrated field and the resulting higher dielectric losses, the radiation losses are negligible in the used frequency band around 300 GHz. Measurement and simulation results which correspond well are shown in Fig. 6(b) for a 180° bend with radii of 5 mm and 10 mm. By decreasing the cross-section of the DWG, the dielectric losses could be decreased (curve shifted to higher frequencies) whereas the radiation losses would be increased.

The dispersion of the DWG must also be considered since a high dispersion would broaden the radar response and decrease the range resolution [10]. The simulated group velocity for the above mentioned cross-section over frequency is shown in Fig. 7. In the used frequency range the curve is nearly constant. For a smaller cross-section the curve would be shifted to higher frequencies and the dispersion would increase. Consequently, the designed cross-section is a compromise of low dielectric losses, low radiation losses and low dispersion.

Since the DWG has a large field of view due to its flexibility, a high gain antenna can be used. An elliptical

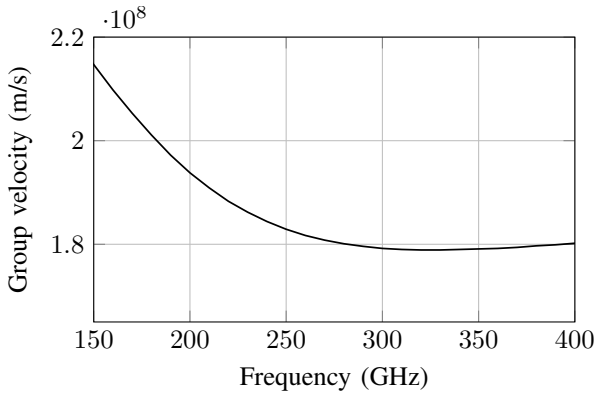

Fig. 7. Simulated group velocity for a rectangular DWG with a cross-section of 432 µm × 864 µm.

lens antenna as proposed in [11] is adapted to the frequency range around 300 GHz. The lens has a diameter of 12 mm (cf. Fig. 8(a)) and a gain of 30.9 dB. The 3-dB beam width is approximately 5° in the H-plane as well as in the E-plane as shown in Fig. 8(b).

A radar measurement of the complete system with a target at 3 m is shown in Fig. 9. Due to the offset of the lens the radar response of the target is shifted to 3.26 m. The zoom window shows the comparison of the target response with (——) and without (- - - -) a flexible front end. Due to the low dispersion, the width of the target response remains constant and a measured range separation of less than 5.6 mm is possible.

VI. Conclusion

In this paper, a 300-GHz radar system with flexible front end is presented to separate electronics and robust antenna in harsh environments. The radar MMIC with a bandwidth of 41.5 GHz is directly connected to the flexible DWG front end. The MMIC in a QFN-like package radiates through the bulk and a silicon lens to focus the wave. The novel transition concept to the DWG encases the entire package and is simply aligned to it and mounted on the PCB. The wave is further focused by multimodal interference to feed the fundamental mode to the DWG. The total transmission loss from MMIC to DWG is 5.5 dB, with only 1.5 dB stemming from the transition. The DWG made of HDPE is low-loss and has an attenuation of 15 dB/m. In addition, it can be bent up to a radius of 1 cm without additional radiation losses. An elliptical lens antenna with a gain of 30.9 dB completes the front end.

Acknowledgment

This work was supported by the Ministry for Science, Research and Arts Baden-Württemberg within the project ZAFH MikroSens.

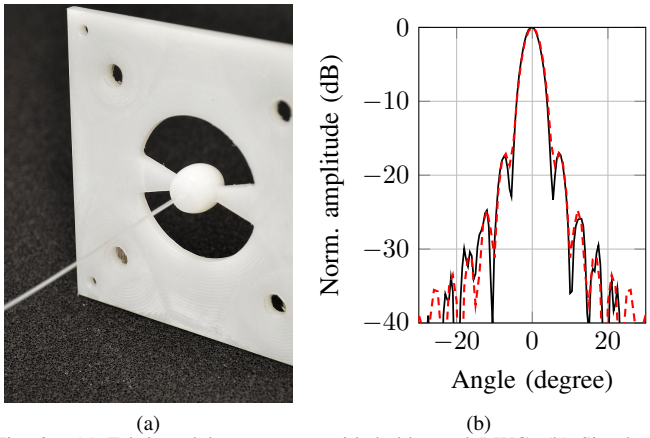

(a) (b)

Fig. 8. (a) Fabricated lens antenna with holder and DWG. (b) Simulated (- - - -) and measured (——) radiation pattern in the E-plane.

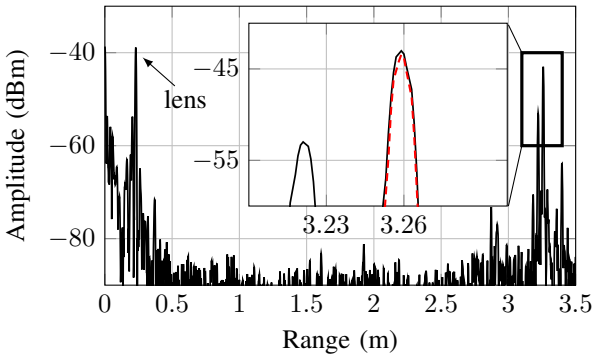

Fig. 9. Range measurement with a corner reflector at 3 m. The zoom window shows the target response with (——) and without (- - - -) flexible front end.

References

[1] J. Grzyb *et al.*, "A 210-270-GHz Circularly Polarized FMCW Radar With a Single-Lens-Coupled SiGe HBT Chip," *IEEE Transactions on Terahertz Science and Technology*, vol. 6, no. 6, pp. 771–783, Nov. 2016.

[2] K. B. Cooper *et al.*, "THz Imaging Radar for Standoff Personnel Screening," *IEEE Transactions on Terahertz Science and Technology*, vol. 1, no. 1, pp. 169–182, Sep. 2011.

[3] P. Hillger *et al.*, "Terahertz Imaging and Sensing Applications With Silicon-Based Technologies," *IEEE Transactions on Terahertz Science and Technology*, vol. 9, no. 1, pp. 1–19, Jan 2019.

[4] M. Geiger *et al.*, "A 160-GHz Radar With Flexible Antenna Used as a Sniffer Probe," *IEEE Sensors Journal*, vol. 17, no. 16, pp. 5104–5111, Aug. 2017.

[5] ——, "Improved Throat Vibration Sensing with a Flexible 160-GHz Radar through Harmonic Generation," in *IEEE/MTT-S International Microwave Symposium – IMS*, Jun. 2018, pp. 123–126.

[6] M. Geiger and C. Waldschmidt, "160-GHz Radar Proximity Sensor With Distributed and Flexible Antennas for Collaborative Robots," *IEEE Access*, vol. 7, pp. 14 977–14 984, 2019.

[7] B. Goettel *et al.*, "Packaging Solution for a Millimeter-Wave System-on-Chip Radar," *IEEE Transactions on Components, Packaging and Manufacturing Technology*, vol. 8, no. 1, pp. 73–81, Jan. 2018.

[8] L. B. Soldano and E. C. M. Pennings, "Optical Multi-Mode Interference Devices Based on Self-Imaging: Principles and Applications," *Journal of Lightwave Technology*, vol. 13, no. 4, pp. 615–627, 1995.

[9] M. Bachmann *et al.*, "General Self-Imaging Properties in $N \times N$ Multimode Interference Couplers Including Phase Relations," *Appl. Opt.*, vol. 33, no. 18, pp. 3905–3911, Jun. 1994. [Online]. Available: http://ao.osa.org/abstract.cfm?URI=ao-33-18-3905

[10] M. Geiger *et al.*, "A Wideband Dielectric Waveguide-Based 160-GHz Radar Target Generator," *Sensors*, vol. 19, no. 12, 2019. [Online]. Available: https://www.mdpi.com/1424-8220/19/12/2801

[11] ——, "A Dielectric Lens Antenna Fed by a Flexible Dielectric Waveguide At 160 GHz," in *11th European Conference on Antennas and Propagation (EuCAP)*, Mar. 2017, pp. 3380–3383.